

## Supporting Information

### Flexible Scintillation Films Based on Ni Co-doped LiLuF<sub>4</sub>:Tb for High-Resolution X-ray and Thermoluminescence Dual-Mode Imaging

Jicong Lin <sup>1,3</sup>, Yushu Dai <sup>1,3</sup>, Jintao Xu <sup>3</sup>, Mengjie Xu <sup>3</sup>, Xieming Xu <sup>2</sup>, Hao Lu <sup>2,\*</sup>, Shaofan Wu <sup>1,2</sup>, Shuaihua Wang <sup>1,2</sup>

1. College of Chemistry, Fuzhou University, Fuzhou, 350108, PR China

2. Fujian Science & Technology Innovation Laboratory for Optoelectronic Information of China, Fuzhou, 350002, PR China

3. Key Laboratory of Optoelectronic Materials Chemistry and Physics Fujian Institute of Research on the Structure of Matter, Chinese Academy of Sciences, Fuzhou, PR China

#### Figures:

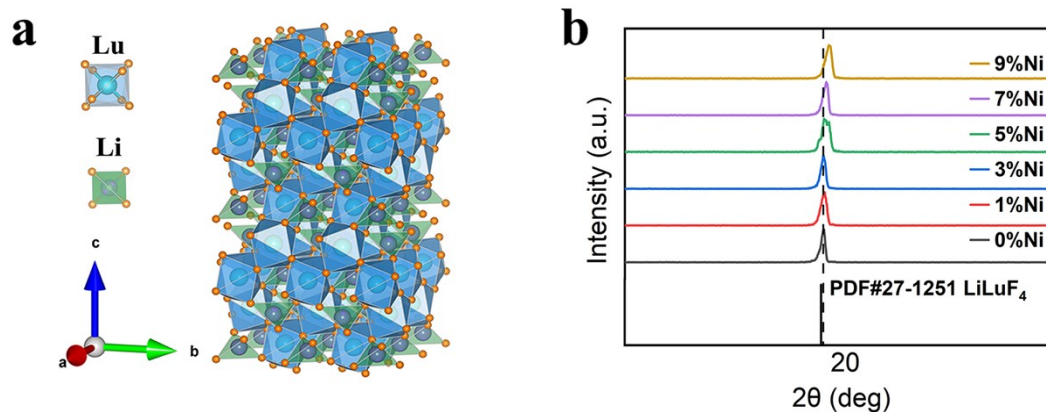


Figure S1 (a) Model diagram of the phase structure of LiLuF<sub>4</sub> microcrystals; (b) XRD of Ni<sup>2+</sup> doped LiLuF<sub>4</sub>:Tb microcrystals;

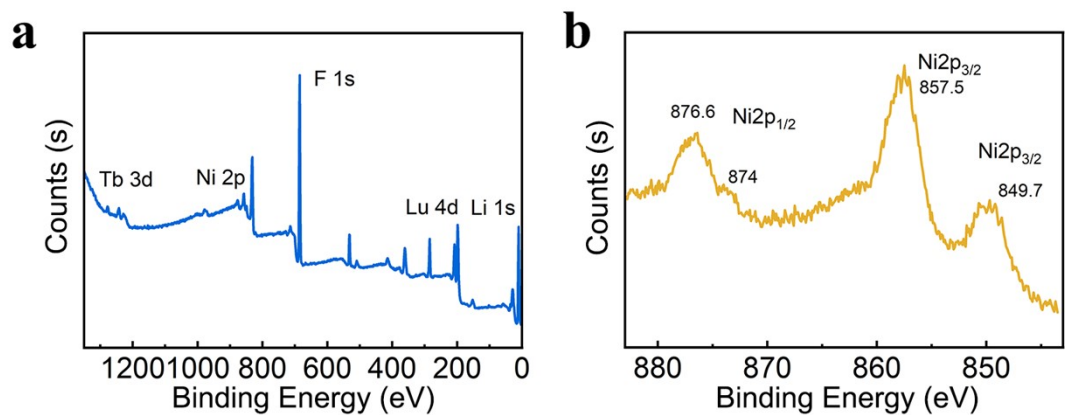


Figure S2 XPS spectral of Ni doped  $\text{LiLuF}_4:\text{Tb}$  microcrystals

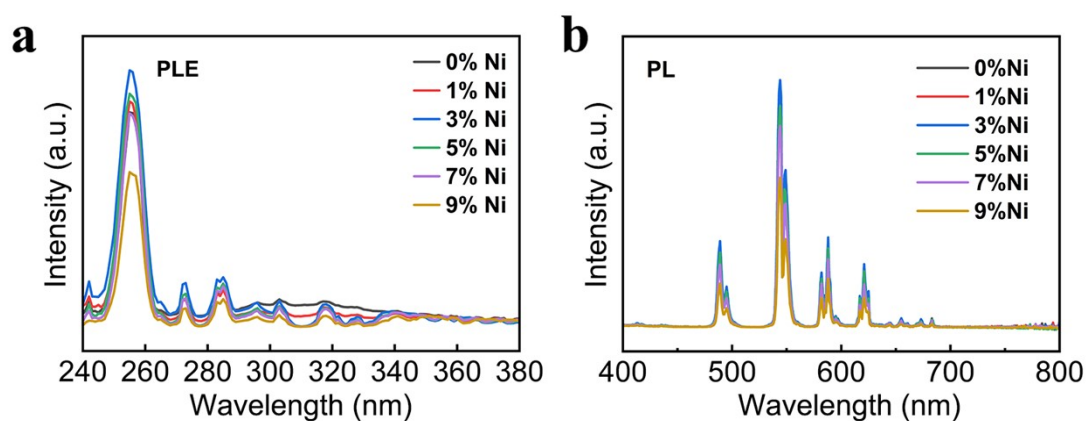


Figure S3 Fluorescence spectral of Ni doped  $\text{LiLuF}_4:\text{Tb}$  microcrystals

(a) excitation spectrum; (b) emission spectrum

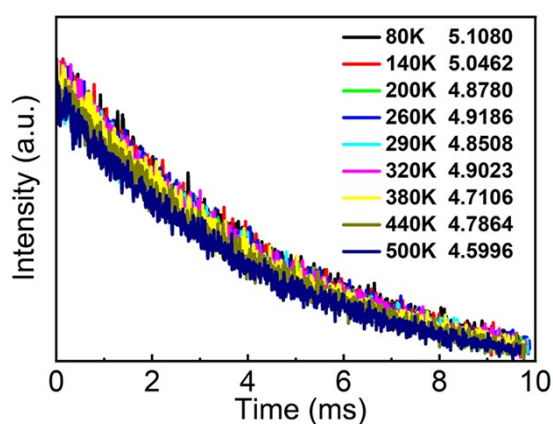


Figure S4 Decay curves of Ni doped  $\text{LiLuF}_4:\text{Tb}$  microcrystals at different temperatures

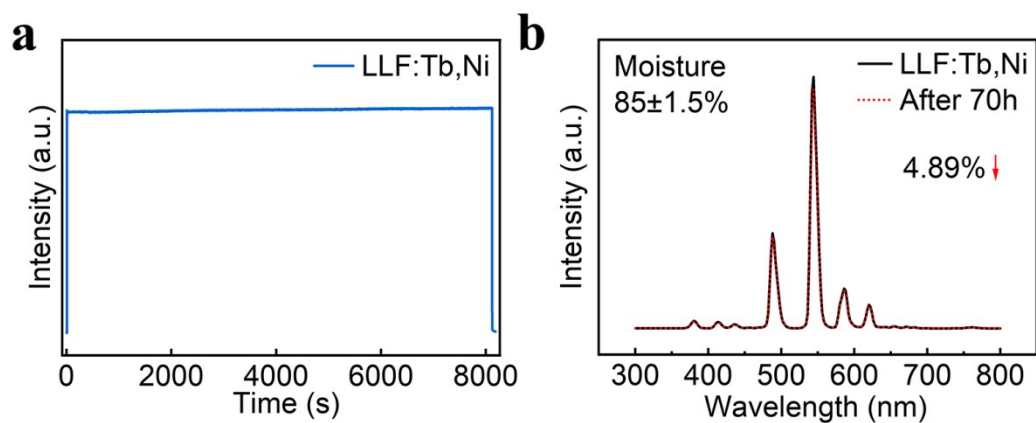


Figure S5 (a) Continuous irradiation stability of Ni doped  $\text{LiLuF}_4:\text{Tb}$  microcrystals; (b) humidity stability of Ni doped  $\text{LiLuF}_4:\text{Tb}$  microcrystals

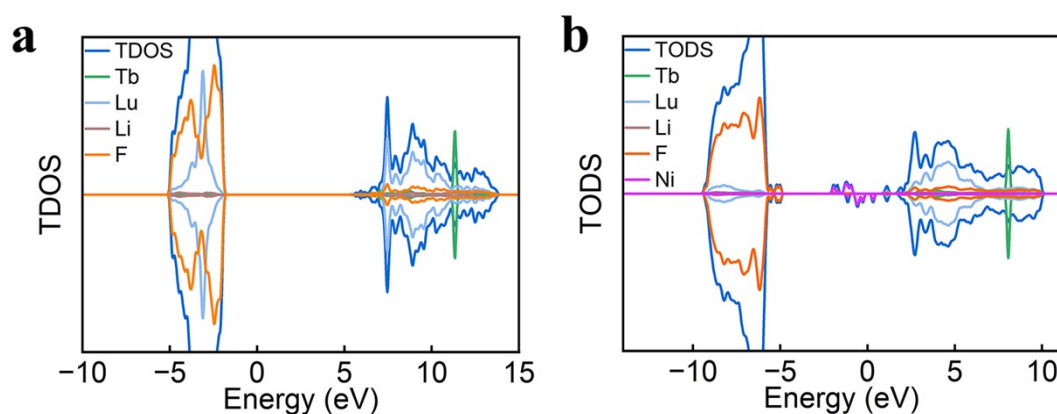


Figure S6 Density of states analysis of (a)  $\text{LiLuF}_4:\text{Tb}$ ; (b)  $\text{LiLuF}_4:\text{Tb,Ni}$

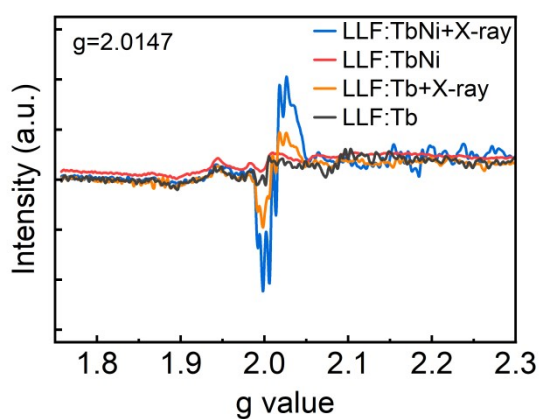


Figure S7 Comparative EPR spectra of  $\text{LiLuF}_4:\text{Tb}$  microcrystals before and after Ni co-doping and X-ray irradiation

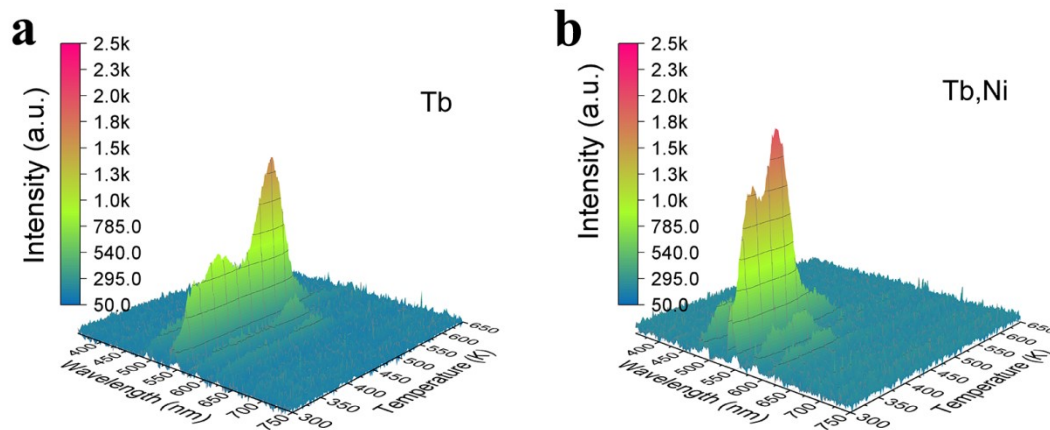


Figure S8 (a) 3D thermoluminescence spectrum of  $\text{LiLuF}_4:\text{Tb}$  microcrystals ; (b) 3D thermoluminescence spectrum of Ni doped  $\text{LiLuF}_4:\text{Tb}$  microcrystals

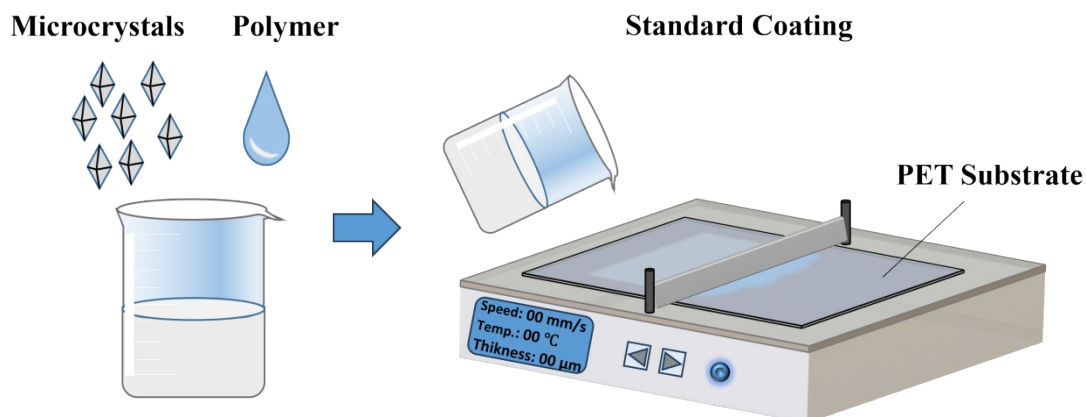


Figure S9 Schematic diagram of  $\text{LiLuF}_4$  microcrystal polymer composite scintillation film preparation

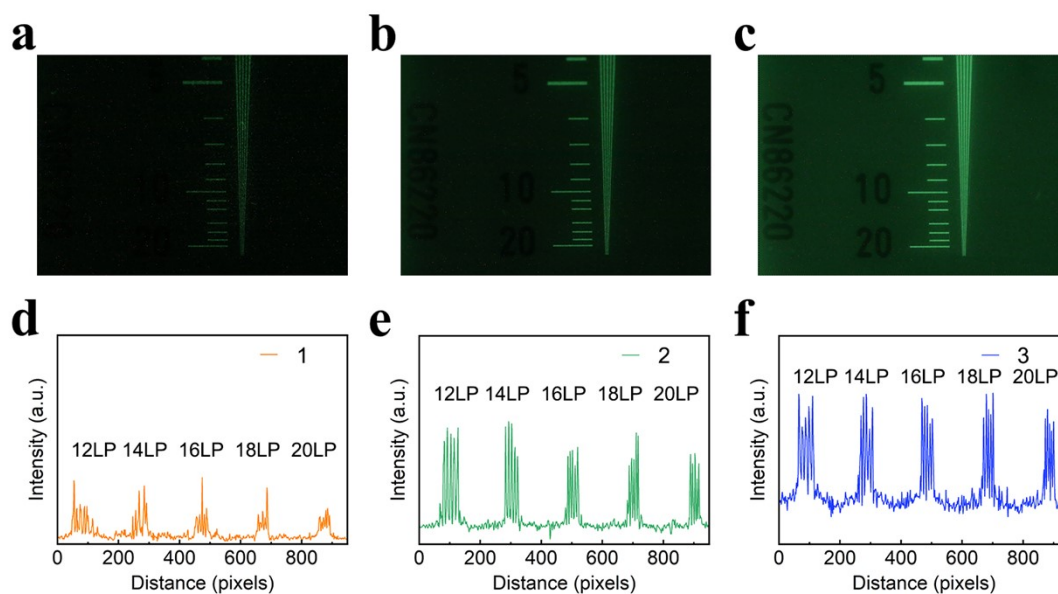


Figure S10 Line-to-card X-ray imaging photographs of  $\text{LiLuF}_4:\text{Tb,Ni}$  composite films with different coating thicknesses. (a)  $50\ \mu\text{m}$ ; (b)  $100\ \mu\text{m}$ ; (c)  $200\ \mu\text{m}$ ; Curve of pixel brightness and darkness change at different line pairs. (a)  $50\ \mu\text{m}$ ; (b)  $100\ \mu\text{m}$ ; (c)  $200\ \mu\text{m}$

**Table S1.** Trap depths in LiLuF<sub>4</sub>:Tb and LiLuF<sub>4</sub>:Tb,Ni microcrystals derived from 2D-TL measurements.

No.	T (K)	LiLuF <sub>4</sub> :Tb		LiLuF <sub>4</sub> :Tb,Ni		
		Trap depths (eV)	Integral area	T (K)	Trap depths (eV)	Integral area
T1	348.85	0.70	36218	334.85	0.67	122264
T2	382.55	0.77	132304	375.05	0.75	106949
T3	473.25	0.95	171489	396.05	0.79	260987
T4	513.85	1.03	28370	450.75	0.90	191925
T5	538.15	1.08	46681	472.05	0.94	92909
T6	-	-	-	531.85	1.06	29359